Schottky signals for longitudinal and transverse bunched-beam diagnostics

F. Caspers

CERN, Geneva, Switzerland

Abstract

Following a brief historical overview on the origin and the evolution of Schottky noise, we discuss applications in the field of beam diagnostics in particle accelerators. A very important aspect of Schottky diagnostics is the fact that it is a non-perturbing method. Essentially statistics based, it allows the extraction of beam-relevant information from rms (root mean square) noise related to the movement of the individual particles. This is also the basis for stochastic cooling. Schottky diagnostics permits one to extract a considerable number of important beam parameters such as the revolution frequency, momentum spread, incoherent tune, chromaticity, and emittance.

1 Introduction

In 1918 the German physicist Walter Schottky (born 23 July 1886 in Zurich) published a paper describing the mechanism of spontaneous current fluctuations in different conductors. This is the origin of the term Schottky noise. The term Schottky noise refers both to thermal noise in resistors and noise in charged particle beams. Additional important contributions from Walter Schottky are the Schottky diode, Schottky defects (in semiconductors) and the Schottky equation (Langmuir–Schottky equation for space charge). In 1915 Schottky invented the tetrode and in 1918 he pioneered the superheterodyne concept. In 1928 the thermal noise in resistors was first measured by J. B. Johnson (Bell Labs) and he discussed his findings with Harry Nyquist who worked at the same laboratory. This is the origin of the term Johnson–Nyquist noise which is more frequently used in the English scientific literature when referring to thermal noise.

An important milestone in accelerator technology was the invention of the stochastic cooling concept in 1968 by Simon van der Meer (Nobel prize shared with Carlo Rubbia in 1984) [1]. Clear Schottky noise signals from a strong coasting (unbunched) beam of protons were observed in 1972 in the CERN–ISR (Intersecting Storage Rings) followed in the same year by the first publication of the cooling idea by Simon van der Meer [2]. In 1975 schemes for pbar accumulation were developed and tested experimentally with protons in 1976 in the Initial Cooling Experiment (ICE). Over the following years a rapid worldwide evolution of beam diagnostics with Schottky noise took place, both for bunched and unbunched beams. Nowadays Schottky diagnostics is a vital element in nearly all large circular machines operating with hadrons and also to a certain extent for electron rings and even linacs. The information extracted in this way allows continuous monitoring of important beam parameters and the control of a number of related machine settings.

2 Shot noise in a vacuum diode

Consider a simple vacuum diode (Fig. 1) where a small number of electrons pass from a heated cathode to the anode [3]. When a single electron is emitted from the cathode and starts moving to the anode

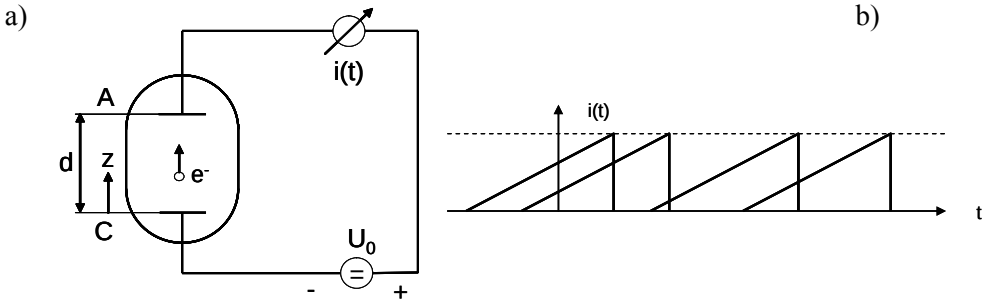

Fig. 1: Normalized spectral density as a function of the transit time angle α (from Ref. [3])

(due to the acceleration voltage U_0) an approximately linear increase of current at the anode is measured. This is due to the dD/dt (D = dielectric displacement) related displacement current which continues as a conducting current when the electron approaches the flat anode. Each of these saw-tooth-like signals [(Fig. 1(b)] has a length τ which is the travel time of the electron from the cathode to the anode. As the individual electrons are emitted in a random manner, these saw-tooth-like signals occur as a non-periodic time function. This is very similar to the time function of acoustic noise originating from little grains falling on a metal plate and is the origin of the term 'shot noise'.

If we assume this diode to be working in the saturated regime (i.e., the anode voltage is high enough that all emitted electrons are accelerated to the anode and there is no space charge cloud near the cathode) then after some derivation, the 'low' frequency spectral density $S_i(\omega)$ of the short circuit current can be expressed as

$$S_i(\omega) = 2I_0 e \tag{1}$$

where e is the elementary charge of an electron with $v_{\mathrm{mean}} = N/\tau$ and I_0 stands for the mean current as defined by $I_0 = ev_{\mathrm{mean}}$.

Obviously the travel time τ plays a very important role for the range of validity of this formula. Typical τ values for vacuum diodes operated at a few hundred volts and a cathode anode spacing of around a centimetre are in the order of a fraction of a nanosecond. This translates to maximum frequencies in the gigahertz range (Fig. 2).

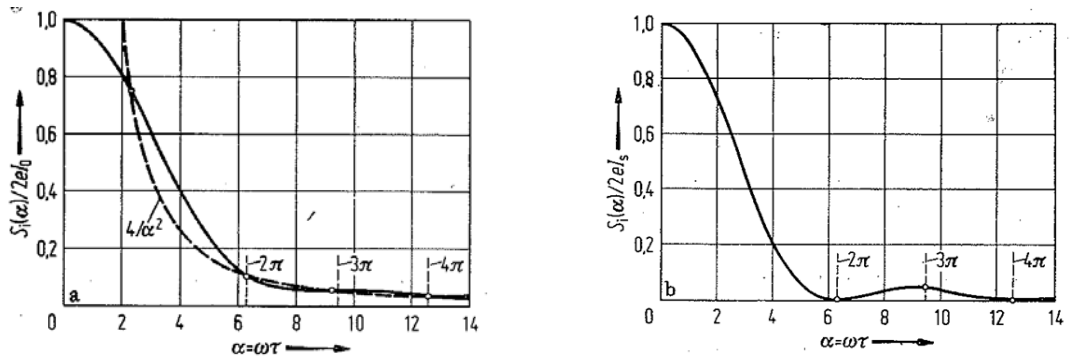

Fig. 2: Normalized spectral density of the short circuit noise current as a function of the transit time angle α (from Ref. [3]); left: for a planar ultra-high-vacuum diode in saturation with current I_0; right: for a solid-state diode in backward bias at saturation current I_s

In a similar manner, starting from the saturated high-vacuum diode, via the vacuum-diode in the space charge region and then applying the theory [4] to a biased and unbiased solid-state diode, one can finally arrive at the noise properties of a linear resistor. This general relation for the open (unloaded) terminal voltage u of some resistor in thermodynamical equilibrium for a frequency interval Δf, which is also valid for very high frequencies f and/or very low temperatures T (K), is given by

$$\overline{u^2} = 4k_B TR \frac{hf / k_B T}{\exp(hf / k_B T) - 1} \Delta f \quad . \tag{2}$$

Here $h = 6.62 \cdot 10^{-34}$ J·s is Planck's constant and $k_B = 1.38 \cdot 10^{-23}$ J/K equals Boltzmann's constant. From this general relation it is possible to write the low frequency approximation ($hf/k_B T << 1$), which is still reasonably valid at ambient temperature up to 500 GHz, as (open terminal voltage, Fig. 3)

$$\overline{u^2} = 4k_b T \Delta f R \ , \tag{3}$$

and for the short circuit current we get accordingly

$$\overline{i^2} = 4k_b T \Delta f / R \ . \tag{4}$$

Note that the factor 4 in Eqs. (3) and (4) often leads to confusion. When **terminating** a noisy resistor with an 'external cold load' (Fig. 3) consisting of a resistor of the same ohmic value (power match) but at 0 K temperature, one can visualize the 'available noise power'. This power delivered to an external load is given by

$$P = k_b T \Delta f \tag{5}$$

and is independent of the value of R. For the power density p per unit bandwidth an even simpler relation is obtained

$$p = k_b T = -174 \text{ dBm/Hz } at \text{ 300 K} \quad . \tag{6}$$

In general 'thermal noise' is given by the random fluctuations of electrons or holes in some conductor with no DC current flow. 'Shot noise' describes the random fluctuations produced by the uncorrelated 'arrival' times of charges with an unidirectional flow.

This relation is also valid for networks of linear resistors with a homogenous temperature between any two terminals. In fact a normal carbon resistor is already such a network of many tiny carbon grains. Equation (6) does not apply to resistors or resistor networks which are not at a homogeneous temperature. In particular, devices which are not in thermodynamical equilibrium such as a DC-biased diode or a transistor connected to some supply voltage are excluded. Such 'active' resistors may have noise temperatures which are considerably below their physical temperature and can be used as a pseudo-cold load in order to avoid bulky and costly cryogenics [4]. As an example one may take the typical TV satellite receiver front-end (LNB = low noise block) where the actual input amplifier has a noise temperature of about 50–70 K in the 10–12 GHz range. For more details on resistor noise see Refs. [5, 6]. In the CERN LEIR machine the concept of pseudo-cold terminations in the 100 MHz range has been applied for strip-line-type pick-ups [7].

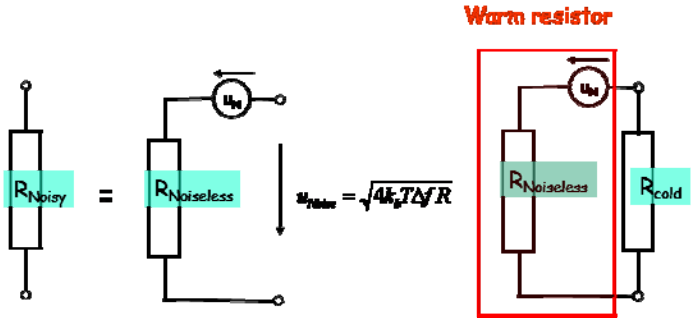

Fig. 3: Visualization of the net power flow from a warm to a cold resistor

3 The field slice of fast and slow beams

Similar to what has been shown for the planar vacuum diode, where the spectrum is a function of the electron velocity and the spacing between cathode and anode, particles in a particle accelerator produce $\beta = v/c$ related spectral modifications in the beam-pipe. This is linked to the fact that virtually all Schottky monitors interact in one way or other with the image current on the inner surface of the beam-pipe. For slow beams the 'field slice' has a certain opening angle (roughly $\sim 1/\gamma$) which causes a 'smear out' of the spatial resolution and thus limits the maximum observable frequency as a function of beam-pipe diameter and γ-value [8]. Figure 4 gives a nice impression of how the 'field slice' contraction for increasing beam velocity enhances the spectral content in the image current towards higher frequencies.

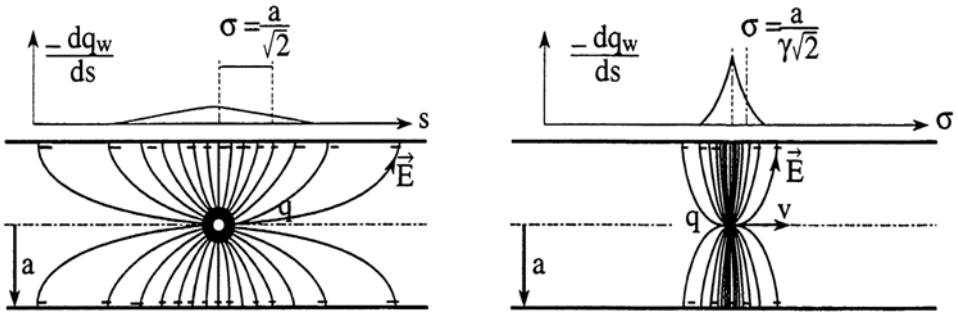

Fig. 4: Electromagnetic field of slow and fast beams (from Ref. [8])

4 Single-particle current

Consider a single particle circulating in some storage ring with a constant frequency $\omega_0 = 2\pi f_0 = 2\pi/T$. This particle will induce a certain signal on some pick-up at its passage time t_k, Fig. 5.

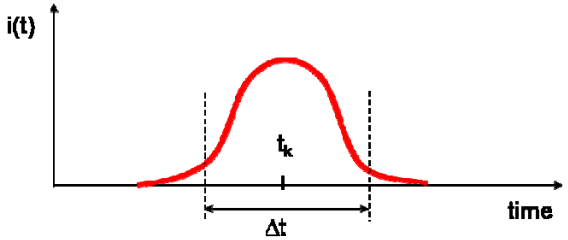

Fig 5: Pick-up signal of a single particle

For a highly relativistic particle and a pick-up with infinite bandwidth this signal should have length $\Delta t \approx 0$ and can be approximated as a Dirac pulse. The signal over m ($m \to \infty$) revolutions can be expressed as

$$i_k(t) = \frac{e}{T}\sum_m \delta(t - t_k - mT) \quad . \tag{7}$$

Applying the Fourier expansion to $i_k(t)$ gives

$$i_k(t) = i_0 + 2i_0\sum_{n=1}^{\infty} a_n \cdot \cos n\omega_0 t + b_n \cdot \sin n\omega_0 t \tag{8}$$

with

$$\begin{cases} i_0 = ef_0 = DC\ current \\ a_n = \cos\ n\varphi_k \quad \text{and} \quad b_n = \sin n\varphi_k \end{cases} .$$

This leads to a corresponding series of Dirac pulses in the frequency domain.

A second particle at a slightly different frequency

$$f_1 = f_0 + \Delta f$$

with

$$\Delta f = f_0 \cdot \eta \frac{\Delta p}{p} \tag{9}$$

returns the situation shown in Fig. 6. The frequency difference Δf at each harmonic of the revolution frequency f_0 then increases proportionally to the harmonic number n.

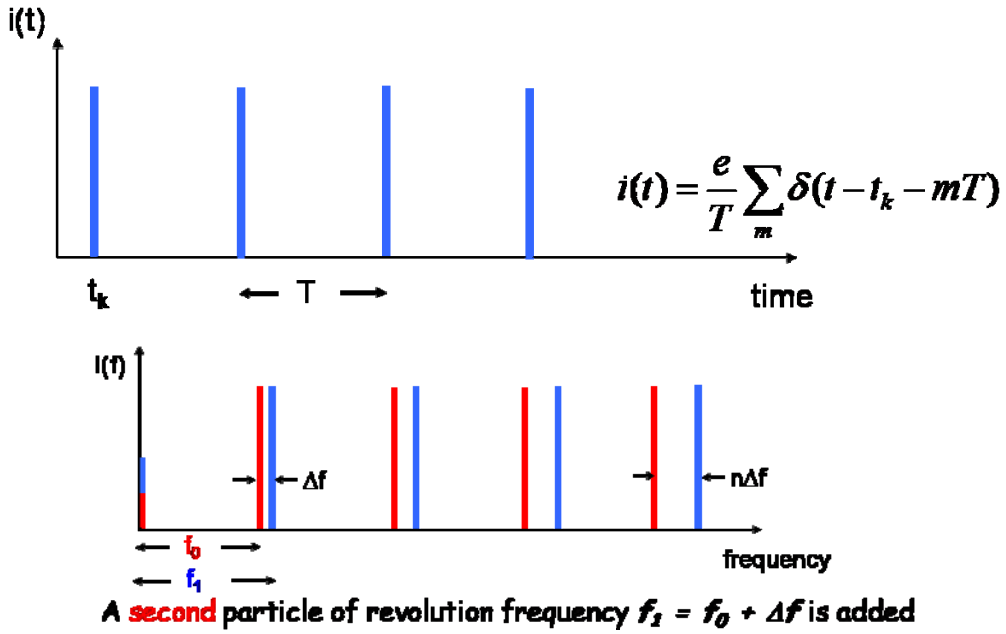

Fig. 6: A single particle and two particles with a slight frequency offset Δf

5 Large number of particles in longitudinal phase space

Now we have to deal with the problem where we have a large number N of particles with (for the moment) equal revolution frequency, but random initial phase:

$$\varphi_k = \omega_0 \cdot t_k \quad .$$

This will result in some amount of mean current:

$$I_0 = N \cdot i_0 = N \cdot e \cdot f_0$$

which is proportional to the number of circulating particles in the machine and which does obviously not depend on the initial phase of each individual particle, and fluctuations caused by the random phases

$$I_t = I_0 + \Delta t$$

where the fluctuations are given by

$$\Delta I = \sum_{n=1}^{\infty} I_n = 2i_0 \sum_{n=1}^{\infty} A_n \cdot \cos n\omega_0 t + B_n \cdot \sin n\omega_0 t$$
$$A_n = \sum_{k}^{N} \cos(n\varphi_k) \qquad B_n = \sum_{k}^{N} \cos(n\varphi_k) \quad . \tag{10}$$

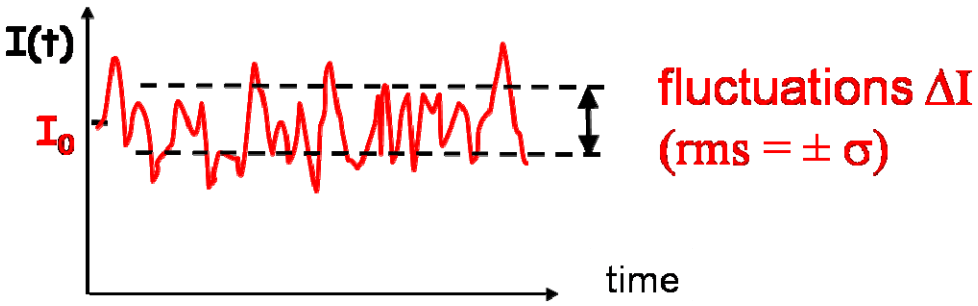

Fig. 7: Illustration of mean current I_0 and fluctuations ΔI

In the total current $I(t)$ the n-th harmonic contains the contributions of all N particles. On a time display one can only recognize a noise trace with some DC offset, Fig. 7. But in the frequency domain distinct bands, (Fig. 8), occupied with noise would become visible. Notice that for the current fluctuations the amplitude ΔI shown in Fig. 7 is a $\pm$ 1σ value and that the peak excursions seen on a scope will be much higher due to the fact that we have a Gaussian amplitude density distribution [9], Fig. 9. One talks often about white Gaussian noise; what does that really mean?

The colour of the noise refers to the spectral distribution over the frequency range of interest by analogy to the colour of visible light:

White light has nearly constant spectral density.

Red light is low-pass-filtered white light.

Blue light is high-pass-filtered white light.

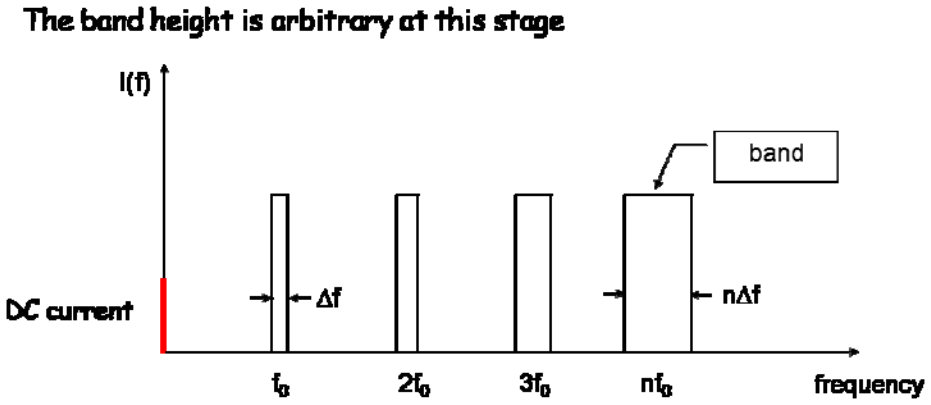

Fig. 8: Spectral density distribution for a large number of mono-energetic particles

Omitting a few intermediate steps in the derivation, one obtains the following expression for the mean square current fluctuations contained in the *n*-th harmonic

$$\langle I_n \rangle^2 = \frac{(2i_0)^2}{2} \sum_{k=1}^{N} \cos^2 n\varphi_k + \sin^2 n\varphi_k = 2e^2 f_0^2 N \quad .$$

Or

$$\langle I_n \rangle^2 = 2e^2 f_0^2 N = 2eI_0 f_0 \quad [\mathrm{A}^2] \quad . \tag{11}$$

This relation, which describes the probable power contribution to the *n*-th Schottky band for a group of *N* **mono-energetic** particles, results in a set of **equal** amplitude lines in the frequency domain, spaced by f_0. There is no dependency on the harmonic number (Fig. 8).

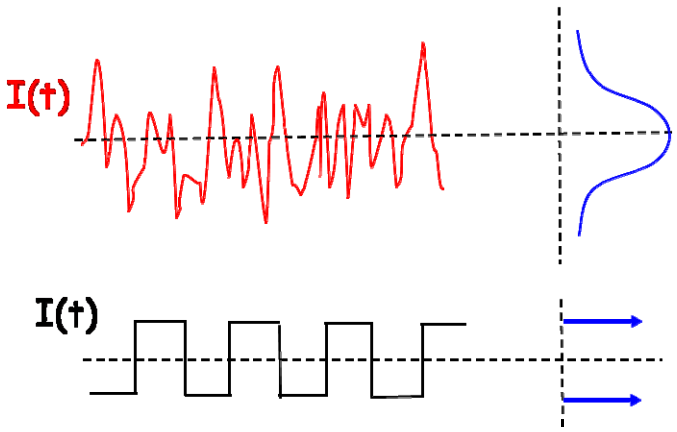

Fig. 9: Illustration of Gaussian amplitude density distribution and non-Gaussian case

The current fluctuations (Fig. 7) now appear as

$$\Delta I = I_{rms} \sum_{n=1}^{\infty} \cos(n\omega_0 t - \varphi_n)$$

with

$$I_{rms} = 2ef_0\sqrt{N} \quad . \tag{12}$$

In the case of ions with charge number Z (i.e. each ion presenting a 'macro-particle' with charge $Z\,e$), the e in the above equation is replaced by $Z\,e$:

$$\langle I_n \rangle^2 = 2(Ze)^2 f_0^2 N \quad . \tag{13}$$

Note that the power in the fluctuations is proportional to Z^2 which means that a single fully stripped uranium ion gives the same signal as about 8500 protons.

Of course it is not realistic to assume that all particles have the same revolution frequency since this would imply either an η-value of 0 or a vanishing momentum spread. Thus we assume a distribution of revolution frequencies as

$$f_0 \pm \frac{\Delta f}{2} \quad .$$

For a subgroup of particles over a very narrow range df the total number of particles N turns to

$$\left(\frac{dN}{df_r}\right) df_r$$

and

$$\begin{aligned} d\langle I_n \rangle^2 &= 2e^2 f_r^2 \left(\frac{dN}{df_r}\right) df_r \\ \Rightarrow \frac{d\langle I_n \rangle^2}{df_r} &= 2e^2 f_r^2 \left(\frac{dN}{df_r}\right) \end{aligned} \quad . \tag{14}$$

The spectral **density** of the noise in the n-th band returns as

$$\left(\frac{d\langle I_n \rangle^2}{df_r}\right) \text{ in units of } [\text{A}^2/\text{Hz}] \quad .$$

After integrating over the band $f_0 \pm \Delta f$ we obtain the total noise power per band:

$$\langle I_n \rangle^2 = 2e^2 f_0^2 N = 2eI_0 f_0 \quad : \tag{15}$$

As an immediate implication we see that the total noise power in each 'Schottky' band is constant. But we also know that the width of the Schottky band is increasing proportionally to the harmonic number, and thus the height must decrease with $1/n$, Fig. 10.

It is very clear from Fig. 10 that when we continue increasing the harmonic number and thus the frequency, at a certain point there will be Schottky band overlap.

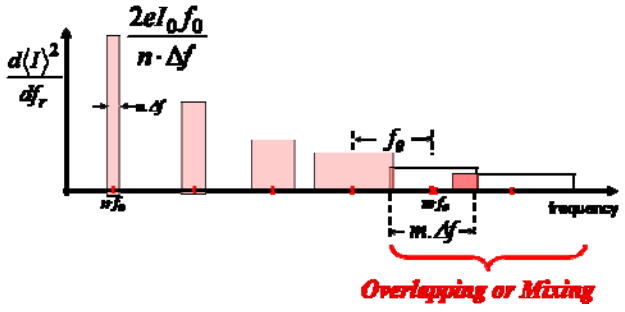

Fig. 10: A realistic picture of longitudinal Schottky bands

From what has been deduced so far for the longitudinal phase space we can already state that the following important beam parameters are measurable with Schottky noise:

The mean revolution frequency

The frequency distribution of particles

The momentum spread

The number of particles

6 Transverse phase space

A single, highly relativistic particle in a storage ring passing through a position-sensitive pick-up with infinite bandwidth generates a series of Dirac pulses (Fig. 11).

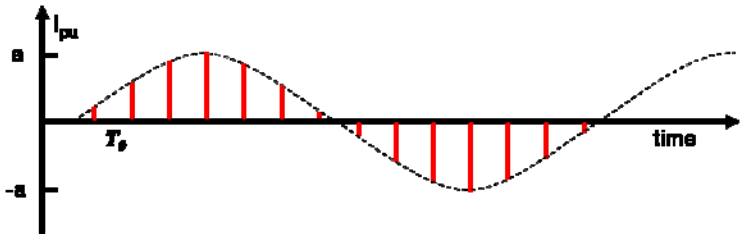

Fig. 11: A single particle with betatron oscillation of amplitude *a* as seen by a transverse pick-up

The betatron motion results in the particle's wobbling around some reference orbit and thus the transverse position changes every turn. This transverse signal is not seen in the sum output of any pick-up structure (e.g. a pair of strip-lines) but is observed in the Delta, or difference, output. The output signal of such a pick-up has two contributions, one related to the longitudinal phase space and another related to the betatron oscillations.

$$i_{pu}(t) = \frac{e}{T}\sum_{n}^{\infty}\delta(t - nT + \varphi_k) \times a_k \cos(q\omega t + \phi_k) \quad . \tag{16}$$

The first term under the sum sign is just the same as already seen in the longitudinal phase space discussion. In addition, however, there is an amplitude modulation of this signal due to the betatron motion. This has a frequency of $q\omega/(2\pi)$, with q being the non-integer part of the betatron frequency and an amplitude a_k representing the oscillation amplitude. The difference response of the pick-up, Δi_{pu}, can therefore be written as

$$\Delta i_{pu} = S_\Delta \times a_k(t) \times i_k(t) = S_\Delta \times a_k \cos(q\omega_0 t + \phi_k) \cdot \left[i_0 + 2i_0 \sum_{n=1}^{\infty} \cos(n\omega_0 t + n\varphi_k) \right] \tag{17}$$

with the term S_Δ defining the transverse sensitivity of the pick-up. The equation for the n-th harmonic then becomes

$$\Delta(i_{pu})_n = S_\Delta \cdot a_k \cdot i_0 \cdot \left[\cos\left((n-q)\omega_0 t + n\varphi_k - \phi_k\right) + \cos\left((n+q)\omega_0 t + n\varphi_k + \phi_k\right)\right] \quad . \tag{18}$$

For N particles in the beam, randomly distributed both in azimuth and betatron phases, averaging Eq. (18) gives

$$\left\langle \Delta i_{pu}^2 \right\rangle = S_\Delta^2 a_{rms}^2 i_0^2 \frac{N}{2} = S_\Delta^2 a_{rms}^2 e^2 f_0^2 \frac{N}{2} \tag{19}$$

representing the total power (in a 1 Ω resistor) in each sideband.

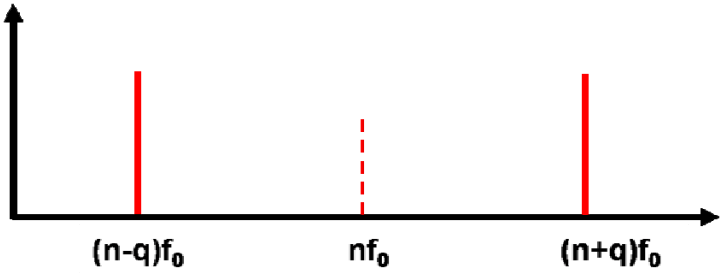

Fig. 12: Illustration of the fractional tune

It can be seen from Eq. (19) that the total power in each band is constant and proportional to the term a^2_{rms} , which for an ensemble of particles is nothing more than the rms transverse beam size and is proportional to the transverse emittance. The width of the sidebands is given by

$$\Delta f_\pm = (n \pm q) \times df \pm f_0 dq \tag{20}$$

where q stand for the fractional tune and dq/Q is the tune spread.

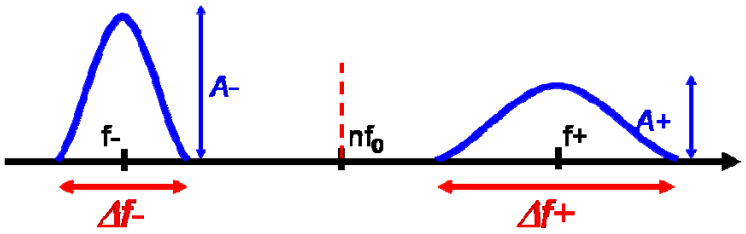

Fig. 13: Example of a Schottky signal with non-zero chromaticity

The fractional part of the tune, q, (Figs. 12,13) can be measured using Eq. (20)

$$q = \frac{f_+ - f_-}{2 f_0} \quad . \tag{21}$$

It should be kept in mind that the situation shown in Fig. 13 assumes that the upper and the lower Schottky band belong to the same revolution harmonic n which implies that the fractional tune is smaller than 0.5. In case the fractional tune is larger than 0.5, the value 0.5 has to be added to the right-hand side of Eq. (21). Without additional information (like doing a small but known tune variation) one cannot tell whether the fractional tune is above or below 0.5.

The tune spread dq/Q is obtained from Eq. (20)

$$\frac{dq}{Q} = \frac{\Delta f_+ - \Delta f_-}{2 f_0 Q} \quad . \tag{22}$$

With the momentum spread dp/p given by

$$\frac{dp}{p} = \frac{1}{\eta} \times \frac{\Delta f_+ + \Delta f_-}{2 n f_0} \quad . \tag{23}$$

Combining Eqs. (22) and (23) and if $n>>q$ it is then possible to calculate the machine chromaticity, ξ :

$$\xi = \left(\frac{dq}{Q}\right) / \left(\frac{dp}{p}\right) \quad . \tag{24}$$

7 Bunched beams

So far the discussion has been limited to the Schottky noise properties of coasting, i.e., unbunched beams. For bunched beams it is necessary to convolute the transverse spectra obtained in the case of an unbunched beam with the synchrotron spectrum related to the motion of particles in the RF bucket. When particles are oscillating in an RF bucket the revolution period $T = T_0$ is no longer constant but modulated periodically in time

$$T(t) = A_s \sin(2\pi f_s t + \psi) \quad . \tag{25}$$

Here A_s stands for the amplitude of the synchrotron oscillation, f_s is the synchrotron frequency, and ψ is some initial phase. Introducing this time dependence into Eq. (1) one obtains, after some manipulations [10]:

$$i(t) = e\, f_o + 2e f_0 \sum_{n=0}^{\infty} \cos\{2\pi n f_0 [t + A_s \sin(2\pi f_s t + \psi)]\} \tag{26}$$

In other words, each single line (cf. Fig. 5) is split up into an infinite number of modulation lines by this synchrotron-oscillation-related phase modulation. The spacing between adjacent lines is equal to f_s. Their amplitude is given by

$$\sum_{p=-\infty}^{n} Jp(2\pi n f_0 A_s) \cos(2\pi n f_0 + 2\pi n f_s + p\psi) \tag{27}$$

with Jp being the Bessel function of order p.

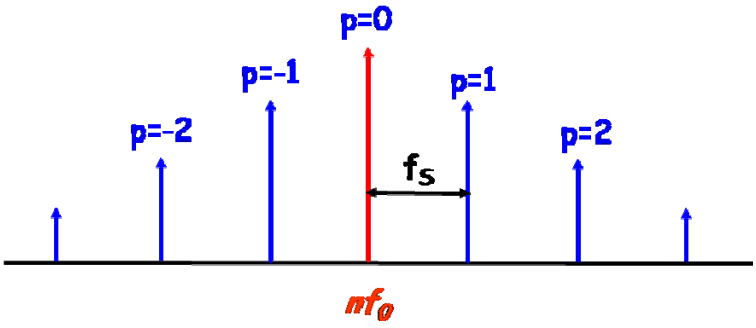

Fig. 14: Illustration of a bunched beam longitudinal spectrum

In a similar way it is possible to obtain an expression [10,11] for the dipole moment D of a single particle travelling in an RF bucket of a circular machine

$$D = a \cos(q 2\pi f_0) e f_0 \cos[2n f_0 t + T(t) \sin(2\pi f_0 t + \psi)] \tag{28}$$

It can be seen that the first cosine term in this equation is related to the amplitude modulation caused by the transverse movement, while the second cosine term represents the phase modulation with f_s. Equation (27) can be further expanded [10] leading to a rather lengthy expression for the amplitude of each particular line.

In short one can say that for the case of bunched beams, each line in the transverse spectrum of the unbunched beam has to be convoluted with the synchrotron-motion-related spectrum. This leads to a fine structure within the distribution shown in Fig. 13. However, the total integrated power is not affected by this synchrotron-motion-related modulation.

8 Discussion of pick-up structures

There is a large variety of pick-up and kicker structures in use for the observation of Schottky signals. The classical example is the basic and well known strip-line structure (Fig. 15) which is frequently referred to as λ/4 structure. However, it can also be operated with a different normalized length. Important properties are

Simple construction

Resonant or non-resonant operation [12] (Fig. 16)

Can be used simultaneously as longitudinal and transverse pick-up

Applicable for highly relativistic as well as slow beams

Can be configured with a low-impedance termination (e.g. 50 Ω) at the upstream end or at low frequencies also as capacitive pick-up with high impedance termination

May be installed in dedicated sections of the machine or inside magnets

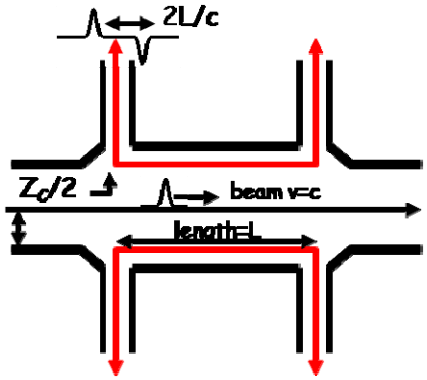

Fig. 15: Basic strip-line pick-up structure

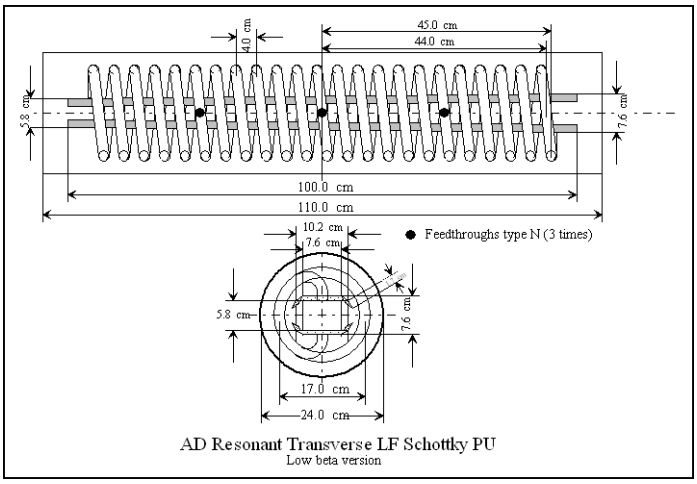

Fig. 16: Resonant strip-line pick-up as used in the CERN AD [12]

Apart from the classical strip-line coupler a number of other devices will be mentioned here:

Shoe-box-type structures are applied for beam position measurements owing to their good transverse linearity; but they are not very sensitive [10]

Printed loop and printed slot couplers (e.g., FNAL and GSI) for stochastic cooling [13, 14] Fig. 19

Ferrite ring structures (up to 500 MHz; CERN 'old' AA) with variable geometry (shutter) during operation for stochastic cooling

Wall current monitor type devices (low sensitivity) mainly for coherent signals

Travelling wave structures with multiple elements such as

- Cascaded strip-lines (super-electrode concept e.g., CERN AD and LEIR) also known as 'n-directional couplers in series [10]
- Travelling wave cavities, e.g., the 200 MHz CERN SPS travelling wave cavities were used at one of their higher order modes (at 460 MHz during the p-pbar project in the SPS as Schottky pick-ups)
- Slotted waveguide structures (FNAL, BNL and LHC) [15,16] Fig. 17
- Faltin type slot couplers [1] Fig. 18
- Cherenkov type dielectric pick-ups (CERN AA around 5 GHz)

Resonant cavities above 1 GHz which are operating on a longitudinal or transverse mode are very sensitive devices. But they may require mechanical displacement during operations in order to follow the beam with their electrical centre. Otherwise, huge revolution harmonics may be induced which are likely to saturate the sensitive head amplifiers of a transverse Schottky signal chain.

Another interesting example is the ferrite-filled cavities operating at a few MHz at room temperature (CERN-AD) [17]. Those cavities exhibit a noise temperature of a few kelvin due to a feedback loop via an ultra-low-noise amplifier trading Q value against noise temperature. The very high longitudinal sensitivity is required for Schottky signal observation on circulating weak antiproton beams as well as intensity monitoring of small p-bar shots in a transfer line.

Schottky noise of just a few charged particles oscillating in a trap is measured by means of resonant capacitive pick-ups. Even single particles can be seen this way. In addition the signals induced in those pick-ups can be used to cool the particles. The energy of the particle movement is simply dissipated in an external terminating resistor.

For the future there are several interesting proposals under discussion such as:

Undulator type pick-ups for optical stochastic cooling

Coherent electron cooling: the electron beam itself acts as a kind of pick-up when travelling together with the hadron beam over a finite length and gives a kind of copy of its fine structure to the electron beam. This fine structure in the electron beam is then amplified similar to a travelling wave tube amplifier and acts back later on the hadrons to be cooled

As we have seen, Schottky signals play a vital role in stochastic cooling since they give a replica of the individual movement of the particles in a beam. Since 'cooling' means 'acting on individual particles' such pick-ups must have a high sensitivity. In certain stochastic cooling systems the particles of the circulating beam just induce on average a single microwave photon (GHz range) per particle and passage through the pick-up structure. It is a nice exercise to work out the numbers for this case.

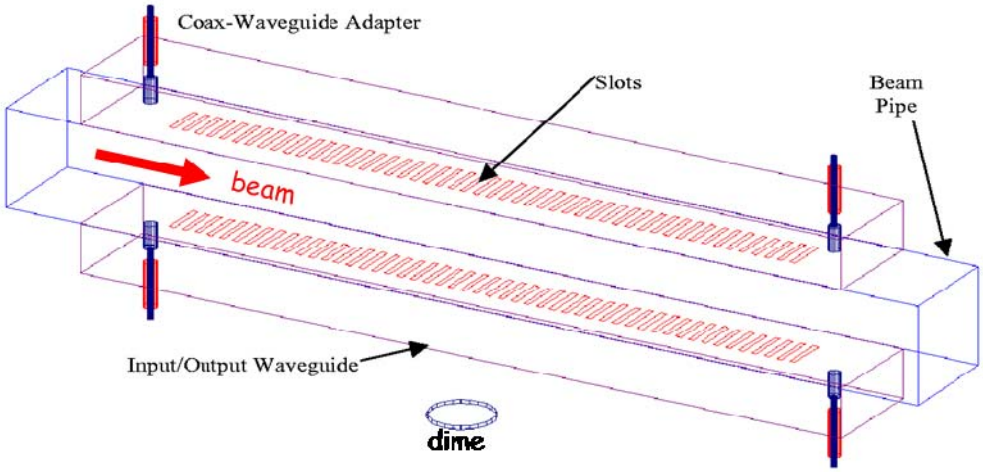

Fig. 17: Slotted waveguide coupler (FNAL [15])

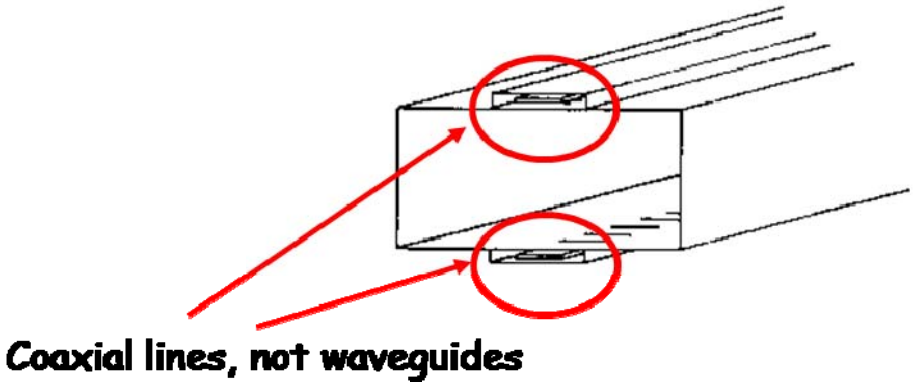

Fig. 18: Faltin type couplers as used in the CERN AA [1]

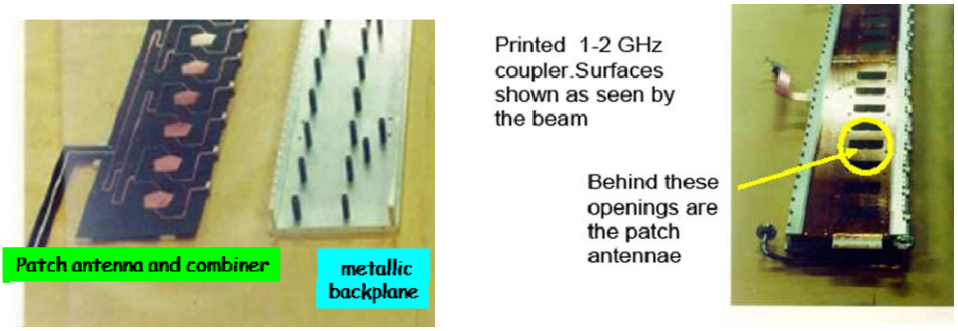

Fig. 19: Printed slot-line structure [14]

For extreme sensitivity requirements, in particular in transverse phase space, the pick-up structure must be cryogenically cooled if there are no other alternatives to reduce the thermal noise level. In addition it may be necessary to follow with mechanically movable electrodes the envelope of the beam e.g., during a cooling process. An example for such a device is shown in Fig. 20. The inner part of the pick-up structure is at about 50 K and the terminating resistors are kept at 20 K [14].

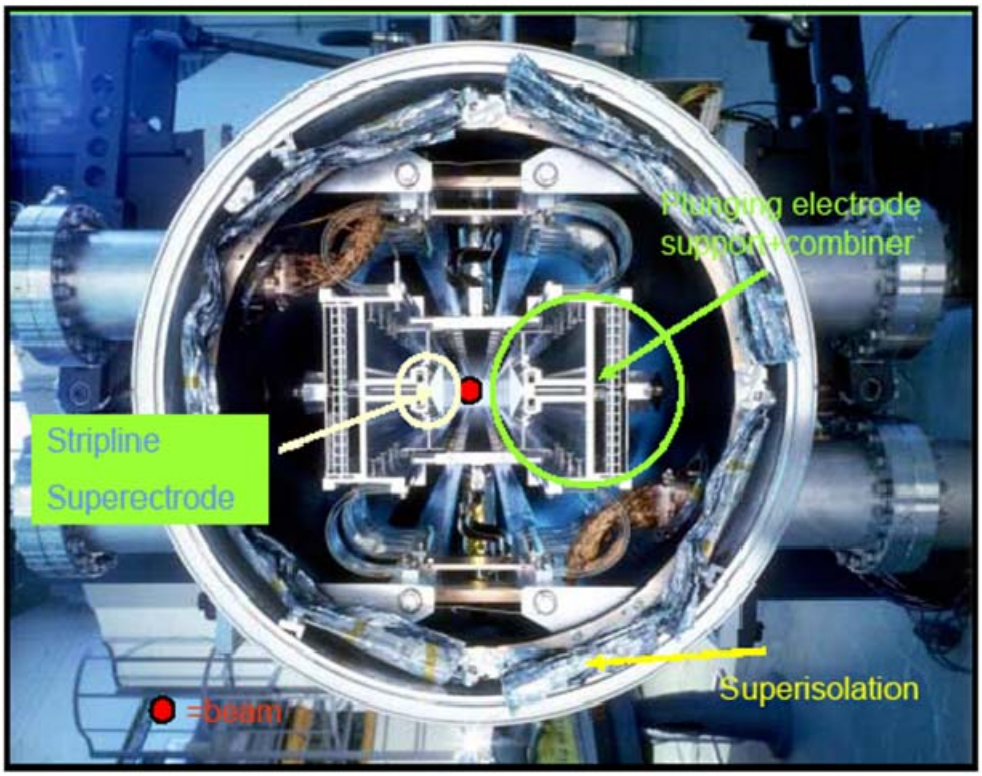

Fig. 20: Example of a cryogenic pick-up with plunging electrodes [14]

9 Signal treatment

The classical method for Schottky signal treatment is done by the implementation of several stages of superheterodyne downmixing as in old-style spectrum analysers. This technique needs a considerable hardware investment but still returns even today the highest instantaneous dynamic range. Such a high dynamic range can be required in case very small incoherent signals have to be detected in the presence of strong coherent lines. Conventional (multiple mixing stage) superheterodyne receivers can achieve more than 120 dB instantaneous dynamic range. Note that the emphasis on instantaneous is rather important and means in other words: no range switching during the measurement process. On the other hand digital signal processing (DSP) type systems are taking over more and more and their architecture can be found in the system structure of modern real-time signal processors, also known as real-time signal analysers or sometimes real-time vector spectrum analysers. In the DSP-style systems the RF signal is digitized with a high vertical resolution close to the front end (although some analog filtering may apply). Subsequently, all the signal treatment like filtering down-mixing and averaging is done by powerful digital processors. In both techniques (classical superheterodyne and DSP) after down-mixing some sort of baseband FFT (Fast Fourier Transform) processing is applied [16, 18]. In certain cases RF gating (Figs. 21, 22) close to the front end may be used in order to separate the incoherent (!) signals of individual bunches. An interesting combination of old and new technologies is analog down-mixing to about 50 KHz and then digitizing the signals with a very cheap soundcard (24 bit vertical resolution), and FFT processing on a laptop computer.

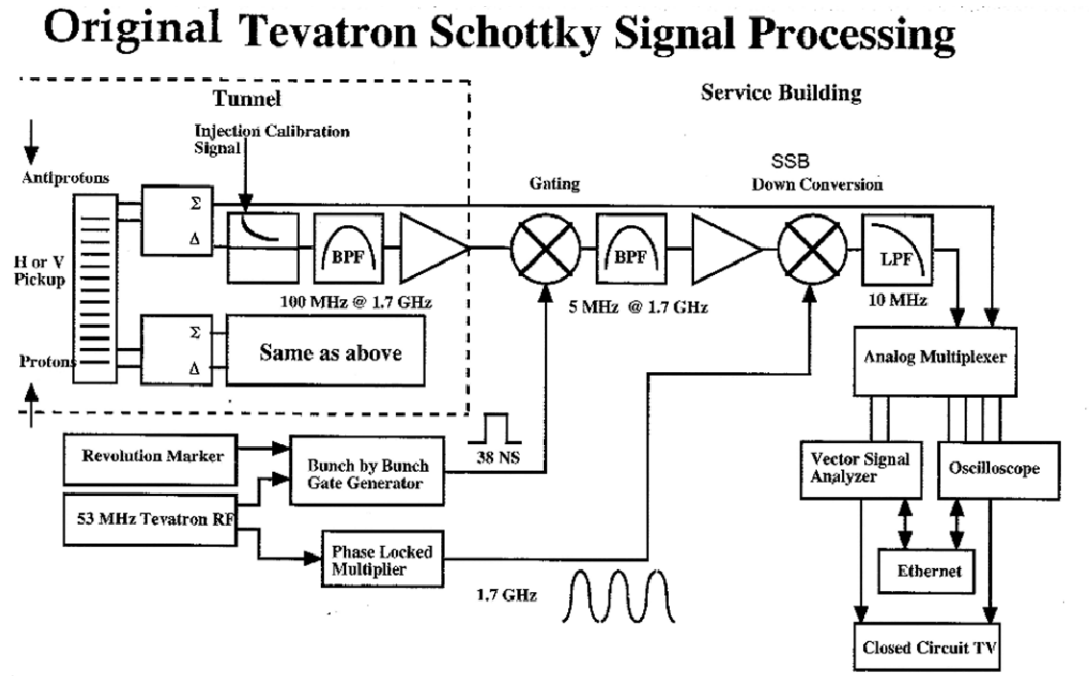

Fig. 21: Example of a Schottky signal treatment chain (FNAL) with gating and single superheterodyne down-mixing [18]

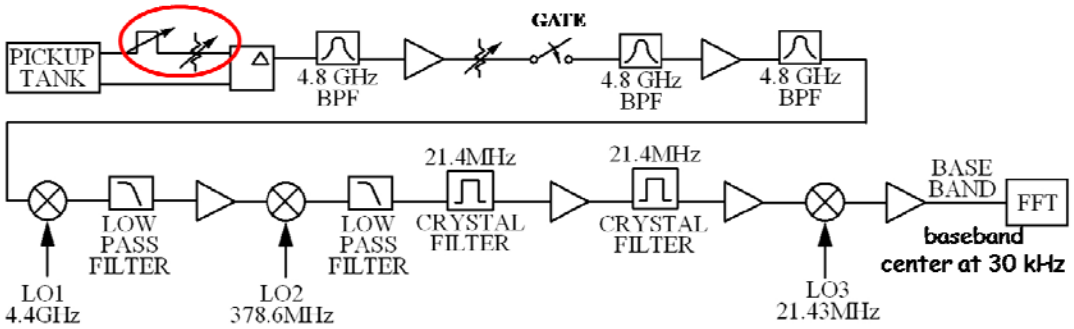

Fig. 22: Example of a Schottky signal treatment chain (LHC) with gating and triple superheterodyne down-mixing [16]

10 Measurement examples

In Fig. 21 we see a nice example from the FNAL Tevatron [18] of how to extract the parameters of interest, namely the tune chromaticity and emittance from measured data. Obviously, the raw measurement data are more or less noisy and require a certain amount of smoothing. As a point of particular interest it should be mentioned that we do not see any (coherent and incoherent) signal related to the revolution harmonic in the middle of this display, which is an indication of having centred the beam excellently in this pick-up. The widths W_1 and W_2, for example, as a ± one sigma value for Δf returns via η the value for $\Delta p/p$. The chromaticity ξ and transverse emittance ε are to be deduced accordingly.

$$q = \frac{1}{2} + \frac{f_2 - f_1}{2 f_{rev}}$$

$$\frac{\Delta p}{p} = \frac{1}{\eta} \cdot \frac{W_1 + W_2}{2\pi f_0}$$

$$\xi \propto \frac{W_1 - W_2}{W_1 + W_2}$$

$$\varepsilon \propto A_1 W_1 + A_2 W_2$$

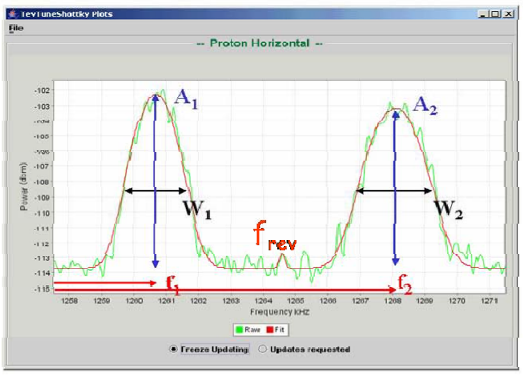

Fig. 23: Measurement example in transverse phase space from the Tevatron [18]

In principle the evaluation of the (incoherent) tune and the momentum spread is rather straightforward with a suitable fitting algorithm, but remember that eventually we need reliable numbers from a basically more or less noisy trace. This kind of parameter extraction is also possible during the ramp (acceleration) provided that in the signal treatment chain the down-mixing is always done to the same baseband frequency (tracking local oscillators).

Since the transverse emittance is proportional to the integrated power of the sidebands (area *A* in Fig. 23) a rough relative measurement is fairly straightforward. But as it becomes clearly visible from Fig. 23 a considerable amount of signal averaging is mandatory with an averaging time in the order of a second. However, for an absolute measurement and for precise results, additional effort is needed. The practical problem there is related to the fact that we must take into account the possibility of gain drifts in the signal processing chain and that we need some kind of calibration such as by doing a wire scanner profile measurement.

Another complementary method [19] takes advantage of the variation of signal strength in the revolution harmonic (incoherent signal) and the betatron sidebands as a function of the mechanical position of the pick-up with respect to the beam. However, the possibility of moving such a pick-up mechanically or displacing its electrical centre by remote control during operation is not always available.

In Fig. 24 we see a typical display of a tune measurement in the baseband [20]. Note that in the left half of the figure we can recognize both coherent and incoherent signal components. In the right half we can recognize the frequency variation of those signals vs time during the ramp. In this case a tracking down-mixing had not been applied.

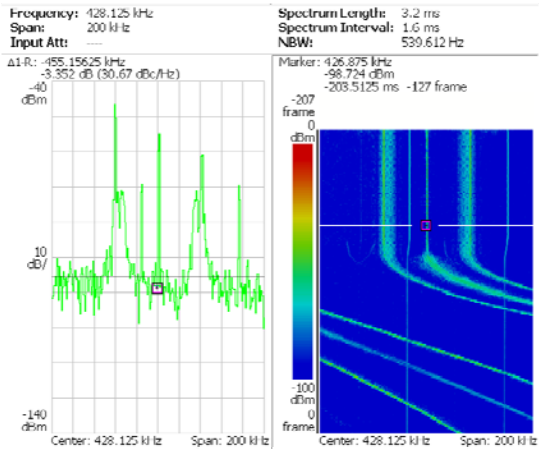

Fig. 24: A typical picture of FFT results at fixed time (left) and during the ramp (right) [20]

11 Conclusions and outlook

We have discussed the basic theory of Schottky noise both for lumped elements like resistors and vacuum tubes but also for charged particle beams in accelerators. The correct understanding of Schottky and thermal noise issues plays a very important role in our everyday life. Applications are found in all kinds of mobile communication devices (cell phone, blue tooth etc.) but also satellite communications such as satellite TV and the GPS system. With respect to particle accelerator applications, Schottky signals are used for different diagnostic purposes but they are also essential for stochastic cooling systems. In this presentation the impact of space charge on Schottky signals was not discussed but it is also a very interesting and challenging issue. For the future we may expect an extension of the frequency range up to optical frequencies and also the development of new ways to extract the information about individual particle behaviour in circulating beams.

12 Acknowledgements

The author would like to thank Jocelyn Tan for important contributions, Rhodri Jones and Trevor Linnecar for inspiring discussions as well as reading the manuscript, and Ed Ciapala for support.

References

[1] S. van der Meer, Stochastic cooling and the accumulation of antiprotons, Nobel lecture 1984.

[2] S. van der Meer, Stochastic damping of betatron oscillation in the ISR, CERN ISR-PO/72-31, Aug. 1972.

[3] O. Zinke and H. Brunswig, *Lehrbuch der Hochfrequenztechnik* (Springer, Berlin, 1974), Vol. 2.

[4] R.H. Frater and D.R. Williams, An active 'cold' noise source, *IEEE Trans. Microwave Theor. Tech.* **29** (1981) 344–347.

[5] http://en.wikipedia.org/wiki/Noise

[6] http://www.ieee.li/pdf/viewgraphs_mohr_noise.pdf

[7] J. Tan, Experimental results from LEIR Schottky system, CERN AB-Note-2008-013, 2008.

[8] A. Hofmann, Physical phenomena used in beam observation, *Third US–CERN School of Particle Accelerators: Frontiers of Particle Beams; Observation, Diagnosis and Correction,* Anacapri, Italy, 1988, M. Month and S. Turner (eds.) (Springer, Berlin, 1989), pp. 367–79 [Lecture Notes in Physics, 343].

[9] S. Chattopadhyay, *Some Fundamental Aspects of Fluctuations and Coherence in Charged-Particle Beams in Storage Rings*, CERN Yellow Report 84–11, October 1984.

[10] T. Linnecar, Schottky beam instrumentation, *in: Beam Instrumentation,* J. Bosser (ed.) (CERN, Geneva, 1992) [CERN-PE-ED 001–92].

[11] D. Boussard, Schottky noise and beam transfer function diagnostics, *CAS – CERN Accelerator School; Fifth Advanced Accelerator Physics Course*, Rhodes, Greece, 1993, S. Turner (ed.) (CERN, Geneva, 1995), pp. 749–82 [CERN-95-06]

[12] V. Chohan *et. al*., Beam measurement systems for the CERN antiproton decelerator (AD). PAC 2001 Proceedings [CERN-PS-2001-053-BD].

[13] http://www-wnt.gsi.de/frs/meetings/hirschegg/program.asp F. Nolden, Fast stochastic cooling of RI beams.

[14] http://www-wnt.gsi.de/frs/meetings/hirschegg/program.asp F. Caspers, Design aspects for stochastic cooling.

[15] R.J. Pasquinelli *et al.*, A 1.7 GHz waveguide Schottky detection system, PAC 2003 Proceedings.

[16] http://adweb.desy.de/mdi/CARE/chamonix/abi_workshop_2007.htm R. Pasquinelli, LARP LHC Schottky (talk).

[17] C. Gonzales and F. Pedersen, An ultra low noise AC beam transformer for deceleration and diagnostics of low intensity beams, PAC 1999 Proceedings [CERN-PS-99-038-RF].

[18] http://adweb.desy.de/mdi/CARE/chamonix/abi_workshop_2007.htm A. Jansson, Schottky observations at the Tevatron (talk).

[19] https://exchange2000.bnl.gov/exchweb/bin/redir.asp?URL=http://www-bd.fnal.gov/icfabd/ *Advanced Beam Dynamics Workshop on High Intensity High Brightness Hadron Beams*, *HB2006*, Tsukuba City, Japan, 2006 (contribution by P. Cameron).

[20] http://adweb.desy.de/mdi/CARE/chamonix/abi_workshop_2007.htm U. Rauch *et al.*, Investigations on baseband tune measurements.